Environmental Science & Technology

Article

pubs.acs.org/est

Spatial and Temporal Trends in Global Emissions of Nitrogen Oxides from 1960 to 2014

Tianbo Huang,[†] Xi Zhu,[†] Qirui Zhong,[†] Xiao Yun,[†] Wenjun Meng,[†] Bengang Li,[†] Jianmin Ma,[†] Eddy Y. Zeng,[‡] and Shu Tao*,[†]

[†]College of Urban and Environmental Sciences, Laboratory for Earth Surface Processes, Sino-French Institute for Earth System Science, Peking University, Beijing 100871, China

[‡]School of Environment, Guangzhou Key Laboratory of Environmental Exposure and Health and Guangdong Key Laboratory of Environmental Pollution and Health, Jinan University, Guangzhou 510632, China

S Supporting Information

ABSTRACT: The quantification of nitrogen oxide (NO_x) emissions is critical for air quality modeling. Based on updated fuel consumption and emission factor databases, a global emission inventory was compiled with high spatial (0.1° × 0.1°), temporal (monthly), and source (87 sources) resolutions for the period 1960 to 2014. The monthly emission data have been uploaded online (http://inventory.pku.edu.cn), along with a number of other air pollutant and greenhouse gas data for free download. Differences in source profiles, not global total quantities, between our results and those reported previously were found. There were significant differences in total and per capita emissions and emission intensities among countries, especially between the developing and developed countries. Globally, the total annual NO_x emissions finally stopped increasing in 2013 after continuously increasing over several decades, largely due to strict control measures taken in China in recent years. Nevertheless, the peak year of NO_x emissions was later than for many other major air pollutants. Per capita emissions, either among countries or over years, follow typical inverted U-shaped environmental Kuznets curves, indicating that the emissions increased during the early stage of development and were restrained when socioeconomic development reached certain points. Although the trends are similar among countries, the turning points of developing countries appeared sooner than those of developed countries in terms of development status, confirming late-move advantages.

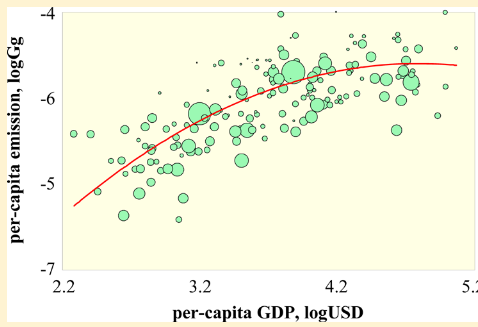

INTRODUCTION

Nitrogen oxides (NO_x, including NO and NO_2) are important components of tropospheric chemistry[1] and play key roles in the formation of ozone and secondary inorganic aerosols.[2] Although NO_x have been among the air pollutants of greatest concern and under regulation in many countries for decades,[3,4] they remain major contributors to current air pollution due to rapid increases in fossil fuel consumption and uneven development among countries.[5]

To quantify the sources and effects of NO_x in the environment and provide necessary information for mitigation strategies, emission inventories of major air pollutants including NO_x have been compiled at global and regional scales.[2,6−13] These data products provide critical inputs to atmospheric chemical transport modeling for quantifying major air pollutants such as $PM_{2.5}$ (particles with aerodynamic sizes less than 2.5 μm) and ozone.[14,15] Among the commonly used global inventories, EDGARv4.3 provides 0.1° × 0.1° spatially resolved annual emission data for anthropogenic and biomass burning sources from 1970 to 2010, with monthly data available for 2008 and 2010.[6] Although monthly data are available in both RETRO[5] and POET[16] for NO_x from both anthropogenic and biomass burning sources, the spatial resolutions are 0.5° × 0.5° and 1° × 1°, respectively, and data after 2000 are unavailable. For atmospheric chemical transport simulation and population exposure assessment, high spatial (0.1° or better) and temporal (monthly or daily) resolutions are preferred.

Among the most important uses of emission inventories of air pollutants is the identification of major emission sources and the development of cost-effective control strategies. In that sense, inventories with detailed source information can help. Recently, a global energy consumption data product (PKU-FUEL) with detailed source information was compiled by our group[17] and used to develop a series of high-resolution inventories for CO, CO_2, BC, OC, $PM_{2.5}$, PM_{10}, SO_2, NH_3, Hg, and polycyclic aromatic hydrocarbons.[17−23] The current version of the product includes detailed source information for more than 80 sources, with 0.1° spatial and monthly temporal resolutions.[24] Compared with the inventory from EDGAR, we focused more on detailed source information for residential sector. In addition, an emission factor (EF, the mass

Received: May 3, 2017
Revised: June 8, 2017
Accepted: June 14, 2017
Published: June 14, 2017

DOI: 10.1021/acs.est.7b02235
Environ. Sci. Technol. 2017, 51, 7992−8000

of a pollutant emitted per unit of activity) database for NO_x from various sources was updated based on a thorough literature review, and country-specific EFs were generated based on either regression modeling[25] or technology division methods.[26] More detailed data are preferred in the future for large countries where regulations vary within countries.

In this study, by using the source strength and EF data, a global NO_x emission inventory with $0.1° \times 0.1°$ spatial and monthly temporal resolutions and covering 87 detailed sources was compiled for the period 1960 to 2014. Monte Carlo simulation was used throughout the process to address and quantify the uncertainties of the estimations. The results were analyzed for geospatial and temporal variations in total emissions, per capita emissions and emission intensities.

■ MATERIALS AND METHODS

Emission Sources and Inventory. A total of 87 detailed sources, including 74 combustion sources, and 13 non-combustion industrial sources, were distinguished (Supporting Information (SI) Table S1). The emission inventory from 1960 to 2014 at a spatial resolution of $0.1° \times 0.1°$ and monthly temporal resolution (for residential, open-field crop residues, and wildfire) was compiled. The total emissions for a given month and specific grid was the sum of the emissions from all individual sources, which was a product of the corresponding fuel quantities (activity strengths) and EFs.

Fuel and Activity Data. Fuel consumption data from PKU-FUEL,[17] which was updated to include more source types and encompass a longer period of time (from 1960−2014), were adopted. The major improvements in PKU-FUEL were that (1) subnational disaggregation energy data based on county (China, the United States, and Mexico), 0.5° (European countries), or province/state (India, Canada, Turkey, Australia, Brazil, and South Africa) were used to reduce spatial biases induced by nonequal per capita energy consumption within large countries[17] and that (2) detailed residential energy consumption data were updated for rural China based on a nationwide energy survey (more than 34 000 households) and solid fuel weighing campaign (more than 1600 households). It was found that the consumption of biomass fuels in rural China reported by IEA were grossly in error.[27] A time-for-space substitution method developed by Chen et al.[24] was applied to simulate monthly variations in residential energy consumption. Monthly data for open-field crop residue burning and wildfire were directly from Global Fire Emissions Databases.[28] Noncombustion industrial activity data were obtained from the World Steel Association,[29] U.S. Geological Survey,[30] and a number of previous studies.[17,22,31] The lime, cement, and coke production activities were spatially allocated based on a previously used procedure.[17] For other noncombustion industrial sources, the activity data were disaggregated based on industrial coal consumption.[19]

EF Data. Over 1000 EFs from various sources were collected from the literature, including those published in recent years. Due to high variations among the EFs for individual sources, an effort was made to generate country and time specific EFs for individual sources. The method was similar to those used previously.[20,23] In brief, for industry, energy production, and motor vehicles, the technology split method was borrowed;[23,26,32] detailed information are provided in SI Tables S2−S6. The method proposed by Bond et al. uses weighted means of EFs of major technologies for a given activity, using fractions of individual technologies as the weighting factors.[26] With limited data available at a global scale, this is the best choice.

Uncertainty Analysis. To address the uncertainty of the inventory, a Monte Carlo simulation was performed. The output contribution of a given source was created after 10 000 repeated computations based on randomly generated fuel (activity) and EF data via a priori distributions with known coefficients of variation (CVs). The energy consumption CVs varied between 5% and 30%, and a log-normal distribution was assumed.[21] The CVs of the EFs were derived from the data collected in this study. The CVs for the technology split ratios were also obtained from our database. To characterize the uncertainty, the results are presented as medians and interquartile ranges.

■ RESULTS AND DISCUSSION

Global Emissions and Source Profiles in 2014. It was estimated that the global total annual emissions of NO_x from combustion and industrial sources in 2014 was 129 Tg. According to the results of the Monte Carlo simulation, the uncertainty range of the estimation, expressed as an interquartile range, was 115−148 Tg. The relative contributions of the activity and EF data to the overall uncertainty were 25% and 75%, respectively, indicating that the EF data were the major source of the uncertainty. The total emissions estimated in this study were close to those reported by EDGAR. For example, the total global anthropogenic emission of NO_x in 2010 was 115 Tg, which is almost identical to the 113 Tg reported in the latest versions of EDGARv4.3 (the latest available data are for 2010).

SI Figure S1 shows the relative contributions of the major source sectors to anthropogenic NO_x emissions in 2010, which are compared with those from EDGARv4.3 (no data for later years). The global source pattern of NO_x emission is very different from those of most other combustion originated air pollutants. Unlike those released as fuel components during combustion such as carbon dioxide (CO_2), sulfur dioxide (SO_2), and metals or generated as incomplete combustion products, including carbon monoxide (CO), organic carbon (OC), black carbon (BC), primary particulate matter (PM), and polycyclic aromatic hydrocarbons (PAHs), NO_x are primarily generated by high temperature reactions.[33] Therefore, power stations and motor vehicles were the most important emission sources of NO_x, contributing 29% and 29% of the total emission at a global scale. The relative importance of these two source categories was one reason that we compiled detailed source data for them. Other important source sectors were navigation (19%) and industry (17%). Although residential fuel consumption plays a significant role in the emissions of all incomplete combustion products such as OC, BC, PM, and PAHs, this sector contributed only 5% of the total NO_x emissions due to the rather low temperatures in residential stoves. Although the total quantity of NO_x emissions estimated in this study is very close to that from EDGAR, the detailed source profiles differ between the two, which can lead to significant differences in spatial distributions. If the sources excluded in our study such as soil emission and manure management are not considered (approximately 10% of the total including direct soil emission, rail transportation, manure in pasture and paddock, and manure management), the contributions of motor vehicles and navigation in our study (29% and 19%) were higher than those of EDGAR (27% and 14%). For motor vehicles, relatively high EFs were used in this

DOI: 10.1021/acs.est.7b02235
Environ. Sci. Technol. 2017, 51, 7992−8000

study for the countries where no control measures are being taken.[32] Our estimate of emissions from motor vehicles in China was higher than that from EDGAR (EDGARv4.3) but generally agree well with those recently reported in a NO_x emission study in China.[2,13] In addition, a recently reported increasing trend in navigation emissions was adopted in this study.[34,35]

Difference among Countries. Of the total emissions, except those from navigation and aviation, which cannot be allocated to specific countries, 23% and 77% were from developed and developing countries (based on definitions of World Bank[36]) in 2014, respectively. The main reason for the larger contributions from the developing countries was their larger populations. In fact, the per capita annual emission of NO_x in developed countries (21.8 kg/cap) was almost twice that in developing countries (13.1 kg/cap), even in 2014, and the differences were even higher in previous years. Globally, the average per capita annual emission was 14.4 kg/cap.

Similar to per capita NO_x emissions, the source profiles were also very different among countries. On average, the relative contributions of motor vehicles (33%) and power stations (39%) in the developed countries were much higher than those (27% and 29%) in the developing countries. This is not surprising because per capita car ownership and electricity consumption in developed countries (0.60/cap and 8994 KWh/cap) were much higher than those in developing countries (0.096/cap and 1967 KWh/cap) in 2014.[37,38] In contrast, residences and industry counted more in developing countries (5% and 23%) than in developed countries (4% and 14%) (SI Figure S2), likely because the contributions of the secondary sector to the economy are relatively high and the efficiencies of residential energy usage are relatively low in developing countries.[23,38]

Similar to the global total, the source profiles for both developed and developing countries revealed in this study differed from EDGAR's (SI Figure S3). For example, excluding other sources (such as trains and fertilization) that were not included in our inventory, the relative contributions of the residential sectors in the developing countries were 7% in both our data and in the EDGARv4.3 data. The differences in the source profiles between the developing and developed countries were strongly associated with socioeconomic development status. In fact, there were significant positive correlations between per capita NO_x emissions from power stations, industry, or transportation and per capita GDP or income ($p < 0.05$). No such dependencies were found for residential emissions.

The log-transformed dependences on per capita GDP and income are shown in SI Figure S4. Although the regression fits using simple linear functions were all statistically significant ($p < 0.05$), the relationships were not necessarily linear. It is especially true that the model cannot be extrapolated to predict future trends, and a leveling-off trend can already be seen for the power generation, industrial, and transportation sectors in developed countries.

If the log-transformed per capita total emissions from power stations, industry, and transportation are plotted against the log-transformed per capita GDPs for all individual countries in 2014, an inverted U curve can be seen in a bubble diagram, and the size of the bubble is proportional to country population (Figure 1). A similar relationship can be obtained by replacing GDP with income. Although incomplete at the high per capita GDP end (right side of the curve), it is a typical environmental

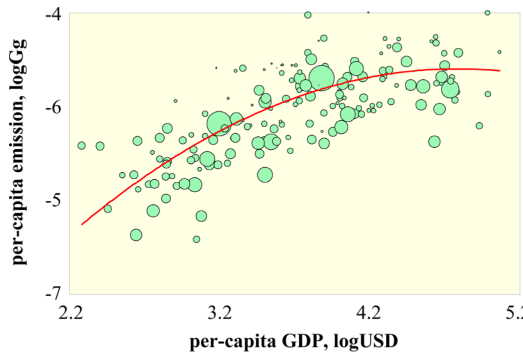

Figure 1. Relationship between per capita emission of NO_x and per capita GDP, both of which have been log-transformed.

Kuznets curve (EKC), and per capita emissions would continue to decrease as per capita income increases above 10^5 USD. By fitting the data with a binomial function, the turning point of per capita GDP was calculated as approximately 60 000 USD. However, the turning point appears to be approximately 10 000 USD based on the date points, rather than the fitting result. In fact, a binomial function may not be a good choice to fit the trend in the first place. Similar trends in PM, SO_2, and BC emissions in various countries have been reported in the literature.[39,40] However, it appears that the turning points for SO_2 and BC are earlier (lower per capita GDP). Technically and economically, controlling NO_x emissions is more difficult than controlling most other air pollutants. Removing gaseous phase emissions is always more difficult than removing particulate phase emissions such as PM and BC, which can be removed gravitationally, electrically or by filtration. On the other hand, SO_2 is more reactive than NO_x in the process. Another reason is that the pollution and adverse impacts of other pollutants such as PM and SO_2 are more visible than those of NO_x.

In addition to per capita emissions, the emission intensities of a country, either defined as anthropogenic emissions of NO_x per quantity of energy consumed (EIe) or per GDP created (EIg), are indicators of energy efficiency or control effectiveness. The EIs of NO_x for individual countries are mapped in SI Figure S5, which reveals even more significant differences among countries, especially the difference between the developing and developed countries. In 2014, the average EIe were 0.20 kg/GJ and 0.13 kg/GJ for developing and developed countries, respectively, and the differences were even larger for the average EIg values, which were 1.41 g/USD and 0.44 g/USD for the developing and developed countries in 2014, respectively. For the developing countries, in addition to relatively low energy efficiencies and productivities, the relatively low outputs of the tertiary industries were an important reason for the relatively low EIe and EIg.

Spatial Distribution. The geographical distribution of the NO_x emission densities in 2014 is shown in Figure 2 at a 0.1° × 0.1° spatial resolution. The source contribution profiles, including six sectors of power generation, industry, residential, transportation, noncombustion industry, and open-field biomass burning (agriculture residue and natural vegetation), are also illustrated as inserted bar charts for 11 major regions: East Asia, South and Southeast Asia, West and Central Asia, Europe, North America, Central America, South America, East and South Africa, West and Central Africa, North Africa, and Oceania. The areas of the pies are proportional to the average

DOI: 10.1021/acs.est.7b02235
Environ. Sci. Technol. 2017, 51, 7992−8000

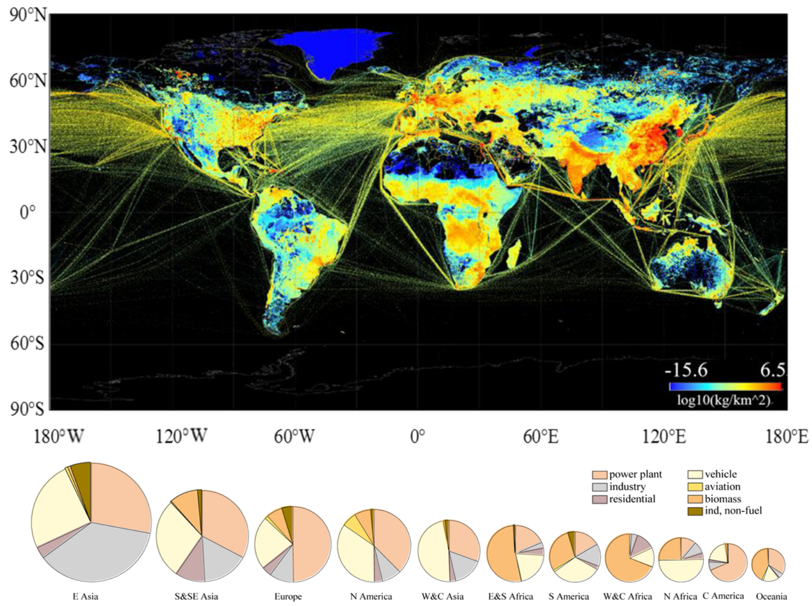

Figure 2. Geospatial distributions of NO_x emission densities, with the exception of aviation in 2014. The source profiles of the emissions in various regions are shown as pie charts.

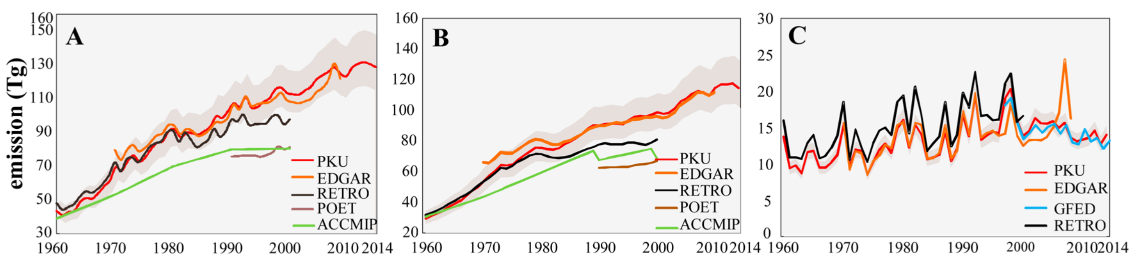

Figure 3. Temporal trends in the total (A), anthropogenic (B), and nonresidential biomass (C) emissions of NO_x from 1960 to 2014. Interquartile ranges (25th to 75th) from the Monte Carlo simulation are shown in shadows. The results are compared with those reported in the literature.

emission densities, and the regions are ranked in descending order from left to right. In general, the geospatial distribution of the NO_x emission densities is very much like those of other major air pollutions such as primary $PM_{2.5}$,[19] black carbon,[22] and PAHs,[21] with extremely high emission densities in eastern China and northern India and relatively high emission densities in Europe and the eastern United States. A primary difference from the distribution patterns of emissions of incomplete combustion products such as BC and OC is the relatively low emissions of NO_x from wildfires in Africa and Brazil. Of the 11 regions, East Asia, Europe, South and Southeast Asia and North America were the top emitters and contributed 69% of the global total. Approximately 30% of global NO_x emissions were from East Asia, in which China is the dominant contributor.

As shown in the pie charts in Figure 2, the emission profiles also differed greatly among the regions. For example, in East Asia, mainly in China, industry, thermal power stations, and transportation ranked highest among all sectors and accounted for 43%, 28%, and 25% of the total emissions, respectively. In India, power stations (44%) and transportation (24%) contributed even more to the total NO_x emissions, followed by industry (21%). In comparison, the top emission sources in North America and Europe were power stations (38% and 50%) and motor vehicles (35% and 23%), whereas the industrial sector was not important due to the higher ratios of tertiary industries and stricter control standards.[38] In most of Africa and Australia, nonanthropogenic sources dominated NO_x emissions, whereas industry, power generation, and transportation provided much smaller fractions than in other regions due to low population densities and rich vegetation coverage. In addition, slow economic development was another cause for Africa. Although the hottest emission regions were in China and India, the relatively high emissions were due to relatively high population densities. As discussed previously, the per capita emissions of NO_x in the developing countries were much lower than those in the developed countries. As a result, after normalizing by population density, the per capita NO_x emissions densities were relatively evenly spatially distributed (SI Figure S6), indicating that the spatial variations in the total emissions were primarily governed by population density. Again, the high per capita emission densities in coastal areas of Australia, south and middle Africa, the southwest United States, and central Brazil were associated with forests or prairie fires in areas with low population densities.

Although cities are often referred as places with severe air pollution, emissions in rural areas are not necessarily low. To distinguish urban and rural emissions, an urban-mask was applied to spatially separate the emissions.[41] It was found that approximately two-thirds of the NO_x emissions occurred in rural areas, with per capita emissions in urban and rural areas of 10.2 kg/cap and 18.0 kg/cap, respectively. According to the results shown in SI Figure S7, per capita NO_x emissions from the industrial and transportation sectors in rural areas were higher than those in urban areas, likely due to the heavy traffic

DOI: 10.1021/acs.est.7b02235
Environ. Sci. Technol. 2017, 51, 7992−8000

on highways and because many industrial parks in developing countries are located in rural areas. Because urban emissions are centralized in relatively small areas with high populations, the adverse impacts on human health in urban areas are much stronger than those in rural regions.

Historical Emission Trends. Like all other major air pollutants, emissions of NO_x increased over most of the years covered in this study. The increasing trend slowed down gradually and did not terminate until very recently. Figure 3 shows historical trends in total, anthropogenic, and non-anthropogenic emissions of NO_x from 1960 to 2014. As shown in Figure 3a, the total worldwide NO_x emissions very probably reached a peak value recently in 2013. Although there were similar decreases that lasted for only one or two years, and data for 2015 and 2016 are not available yet, the decreasing trend since 2013 suggests a turning point, which is also supported by other evidence. For example, coal consumption in China has continuously decreased since 2014,[42] and serious and effective efforts have been undertaken in China toward denitration at all major power plants.[43] Moreover, the global average per capita GDP was approximately 10 000 USD in 2013,[38] similar to the results shown in Figure 1, which were derived based on per capita NO_x emissions from country data. Nevertheless, the turning point in the historical trend of total NO_x emissions was later than those of several other major air pollutants such as SO_2,[44] BC,[22] and PAHs.[21] Another piece of evidence is that some historical variations were often caused by random changes in wildfires such as the decreases from 1970 to 1971 and 1992 to 1993. On the other hand, nonanthropogenic emissions actually increased from 2013 to 2014 (Figure 3c), against the decrease in anthropogenic emissions. In terms of origins, NO_x, which is formed at high combustion temperatures,[33] is very different from most other air pollutants, which are either incomplete combustion products formed during burning processes such as CO, BC, OC, and PAHs or released fuel components, including SO_2 and metals. The declining emissions of incomplete combustion products in recent years are largely due to transitions in energy mixes in China and other developing countries,[45] and the reduced emissions of SO_2 can be attributed to desulfurization facilities that have been extensively installed in power stations and industrial facilities.[46] In comparison, efforts on NO_x emission control are relatively slow. In addition, denitration of automobile tail gases is neither easy nor cheap. Fortunately, the continuously increasing trend has finally been contained in recent years, mainly due to stricter controls on emissions from power generation and motor vehicles in large developing countries such as China,[43] whereas the emissions in developed countries occurred decades ago. For example, China began to adopt EU emission standards for motor vehicles in 2000 and stricter NO_x emission standards for power plants (GB13223−2011) and the iron and steel industry (DB13/2169−2015).[47,48] Although the emissions from non-anthropogenic sources (Figure 3c) accounted for a rather small fraction of the total emissions (10−20%), they contributed significantly to the fluctuations among years, whereas the anthropogenic emission changed more smoothly over years (Figure 3b). The variations in wildfire emissions were very much climate dependent. Typical examples include high emissions during the periods of 1982−1983 and 1991−1994, when strong EI Nino resulted in high temperatures and drought in South and East Africa, which favored the occurrence of wildfires.[49,50]

For comparison, the trends of NO_x emission reported by other sources such as EDGARV4.3, POET,[16] RETRO,[5] and ACCMP[10] for anthropogenic sources and EDGARV4.2,[51] GFED, and RETRO for nonanthropogenic sources are also shown in Figure 3. The estimated total global NO_x emissions during the period from 1960 to 2008 are similar to those from EDGARv4.2, especially after 1980. As discussed above, although the total emissions are close to each other, there are significant difference in source profiles between our inventory and EDGAR. This is true not only for 2010 but also for other years. Without data from railway and soil in our study, emissions from 1960 to 1980 in our inventory were slightly lower than those from EDGAR. After 1980, however, the differences were made up by relatively fast increases in emissions from navigation and transportation due to inclusion of latest published EF data.[34,52] Although the emissions in 1960 estimated by this study agree well with those in ACCMIP, the increase trends are very different. By the year 2000, the NO_x emission in ACCMIP was approximately 25%−30% lower than our data. The main reason is difficult to identify without detailed source and EF information for ACCMIP.[10] This is also true for POET.[16] The temporal change trend in NO_x emissions has been captured by numerous studies using satellite remote sensing image.[53−56] Those studies suggest that NO_x emissions for China increased at rates from 7.3 to 8.7% during 1996 to 2006, consistent with our estimation of a 6.4% increased rate during that period. Similar trends have been revealed using remote sensing data from GOME and SCIAMACHY for various regions, including continuous reductions over western Europe and the United States from 1996 to now[54,57] and decreases starting in recent years in China.[58]

SI Figure S8 shows the temporal trend in the NO_x emissions from major global sectors, the developed countries, and developing countries. The trends in total emissions are shown in Figure S8a−c, and those for the relative contributions of different sectors are shown in Figure S8d−f. It is interesting to observe the rapid growth in emissions from navigation throughout the world. The trend agrees with the rapid increases in the number of ships and quantity of fuel consumed, likely due to accelerated globalization in the past.[34] There are significant differences in the temporal trends between the developed and developing countries (those from navigation were not assigned to either developed or developing countries). The emissions in developed countries had leveled off since early 1970s and declined in recent decades, largely due to stabilization followed by reductions in emissions in the transportation (motor vehicles) and energy production sectors. In developed countries, NO_x control technologies have been extensively adopted in coal-fired power plants,[59] and strict regulations on vehicular emissions have been implemented in recent decades.[60−62] In developing countries, however, emissions from most sectors have generally increased continuously up to recent years. The total annual anthropogenic emissions of NO_x increased almost an order of magnitude from 7.39 Tg to 67.8 Tg during the study period, in accordance with rapid economic development and the expansion of personal car fleets.[63,64] Among all sectors, the only exception was residential emissions, which remained unchanged over the years. It appears that the increase caused by population growth was compensated by the residential energy mix transition from solid fuels to clean energy.[65] The relative contribution of this sector has decreased due to increases in other emissions. In addition, motor vehicle emissions in

DOI: 10.1021/acs.est.7b02235
Environ. Sci. Technol. 2017, 51, 7992−8000

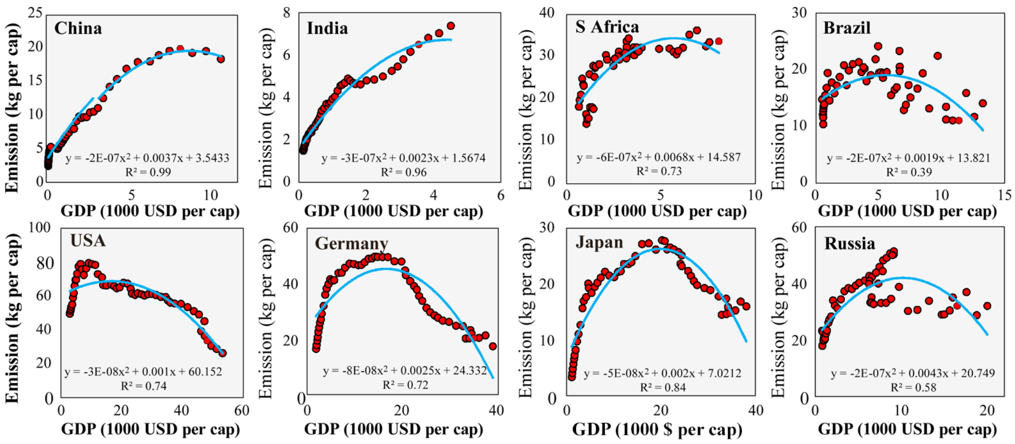

Figure 4. Dependence of per capita NO_x emissions on GDP for representative countries. The trends are fitted with binomial equations.

developing countries appear to have reached a turning point in 2013−2014, driven primarily by regulatory efforts in China.[66,67] For both developed and developing countries, the relative contributions of power and industrial sources are increasing. Fortunately, rapid increases in the selective catalytic reduction in Chinese power plants led to a sharp decrease in that sector.[43]

The temporal trends of EIe and EIg differ from the total emissions. EIg has decreased approximately 90% from 11.0 g/USD in 1960 to 0.92 g/USD in 2014 (SI Figure S9), primarily because of increases in production efficiency. For EIe, however, the value increased from 0.19 kg/GJ in 1960 to 0.23 kg/GJ in 1983 and then decreased back to 0.18 kg/GJ in 2014. The fluctuation was driven primarily by an energy mix transition and increasing mitigation efforts. There were also significant differences between the developing and developed countries. For EIe, a rapid decrease after 1990 can be found for the developed countries, whereas the much slower decrease for the developing countries did not occur until the turn of the century. For EIg, the trends for the two country categories were very similar but with different absolute values.

The dependencies of the per capita emissions of NO_x on the per capita GDPs are shown in Figure 4 for eight representative countries: the United States, Germany, Japan, Russia, China, South Africa, Brazil, and India. Similar to the relationships among countries for a single year, the trends for the individual countries over years generally also had inverted U-shapes, indicating that the relationships between emissions and per capita GDP followed the EKC. Although the data for India are monotonic, it is very likely the left half of the EKC, and the turning point has not yet been reached. It is interesting to compare those countries' turning points. For the three developed countries, the turning points appear around per capita GDPs of 9200 USD (The United States), 14 300 (Germany), and 20 100 USD (Japan). Many efforts have been made to reduce emissions of various air pollutants, including those of NO_x, in those countries since the 1970s. For example, the NO_x emission standard for diesel vehicles has been reduced from 13.4 g/kwh (grams per kilowatt-hour) in 1979 to 0.27 g/kwh in 2010 in the United States, resulting in significant reductions in emissions.[60,68] Similarly, emission standards for motor vehicles have evolved from EU-I to EU-VI in European countries,[32] and the strict JC08 standard was introduced in Japan.[69] In comparison, the turning points of the countries in economic transition were approximately 8100 USD (China), 9100 (Russia), 6900 USD (South Africa), 5000 (Brazil), and >1600 USD (in India, that point has not yet been reached). In addition, at the turning points, the per capita emissions in the developed countries (80, 50, and 28 kg for the United States, Germany, and Japan) were also generally higher than those in the developing countries (20, 36, and 24 kg for China, South Africa, and Brazil). The significant difference between the developed and developing countries suggests that the latter had learned lessons and borrowed control technologies from the former, and the late-move advantage has been well demonstrated. For example, a Chinese standard for motor vehicle emissions (GB 18352.5−2013), which is similar to Euro V, is to be introduced in 2017.[70] Although it is approximately eight years later than in European countries, the per capita GDP that year in China was approximately 9000 USD, equivalent to those in the UK in 1977, Germany and France in 1978, and Italy in 1986. There have been previous studies on the EKCs of the emissions of a variety of air pollutants, including NO_x, and the turning points reported in those studies varied from 12 000−21 800 USD for various countries.[40,71]

Intra-Annual Variations. By assuming that the NO_x emission seasonality is dominantly governed by the intra-annual variations in residential fuel consumption and open-field biomass burning sources, the monthly NO_x emissions were generated and included in the inventory based on monthly residential energy consumption[24] and open-field biomass burning data.[28] The monthly total NO_x emission data, which have a 0.1° × 0.1° spatial resolution from 1960 to 2014, can be downloaded from our Web site (http://inventory.pku.edu.cn). Because the monthly residential energy consumption was quantified based on a set of social-economic parameters using a space-for-time substitution method,[24] daily data can also be generated, if only the daily data for parameters such as heating-degree-day and cooling-degree-day can be obtained. For remote sensing based open-field biomass burning, daily data are also available.[28] In fact, the daily data are necessary for atmospheric transport modeling. Of course, those data are too large to be uploaded.

The intra-annual variations in the NO_x emissions originated from seasonal variations in wildfires, open-field straw burning, and household heating, and the variations were spatially dependent on variations in harvest seasons, wildfire seasons, and heating seasons in different regions. The spatial distributions of such seasonality are shown in SI Figure S10 as coefficients of variation (CVs) for open-field biomass burning (wildfire and agricultural waste) emissions (SI Figure

DOI: 10.1021/acs.est.7b02235
Environ. Sci. Technol. 2017, 51, 7992−8000

S10a) and residential emissions (Figure S10b). The distribution patterns of the emissions from wildfires and burning open-field straw generally agree with those observed in satellite images, reflecting the distributions of thick forests (such as the taiga in Russian Siberia), grasslands (such as the savannahs in East Africa and central Brazil), and crops (such as in eastern China).[28] However, high variations in residential emissions occurred in high altitude regions, either north or south, especially in densely populated areas. A similar pattern has been reported in the literature.[9]

Citing a few examples, SI Figure S11 shows monthly variations in NO_x emissions worldwide (SI Figure S11a) and in China (SI Figure S11b), Australia (SI Figure S11c), and Brazil (SI Figure S11d) in 2014. Because the seasonalities of the emissions are driven by those of the residential (heating in winter), agricultural (open-field crop residue burning), and wildfire (forest and prairie fires) sectors and the NO_x is predominantly from power station, motor vehicles, and industry, there were slight variations in NO_x among the months. For example, the difference between the highest and lowest monthly emissions was only 7% globally, which is very different from the monthly variations in incomplete combustion products such as PM, BC, and OC, which are primarily or dominantly from the residential sector.[17,19,22] For individual countries, however, strong seasonality can be found. For example, very high NO_x emissions appeared during the fire seasons in Australia and Brazil.

■ ASSOCIATED CONTENT

Supporting Information

The Supporting Information is available free of charge on the ACS Publications website at DOI: 10.1021/acs.est.7b02235.

> List of individual sources, detailed information on EFs, relative contributions of major source sectors, relationship between emissions and per person GDP/incomes, geographical distributions of per capita emissions and nonresidential biomass and residential emissions, time trends of emissions, emission intensities (PDF)

■ AUTHOR INFORMATION

Corresponding Author

*Phone/fax: +86-10-62751938; e-mail: taos@pku.edu.cn.

ORCID

Shu Tao: 0000-0002-7374-7063

Notes

The authors declare no competing financial interest.

■ ACKNOWLEDGMENTS

This work was supported by the National Natural Science Foundation of China (41390240, 41571130010, and 41629101).

■ REFERENCES

(1) Irie, H.; Sudo, K.; Akimoto, H.; Richter, A.; Burrows, J. P.; Wagner, T.; Wenig, M.; Beirle, S.; Kondo, Y.; Sinyakov, V. P.; Goutail, F., Evaluation of long-term tropospheric NO2 data obtained by GOME over East Asia in 1996–2002. *Geophys. Res. Lett.* **2005**, *32*, (11). DOI: 10.1029/2005GL022770.

(2) Zhang, Q.; Streets, D. G.; He, K.; Wang, Y.; Richter, A.; Burrows, J. P.; Uno, I.; Jang, C. J.; Chen, D.; Yao, Z.; Lei, Y., NOx emission trends for China, 1995–2004: The view from the ground and the view from space. *J. Geophys. Res.* **2007**, *112*, (D22). DOI: 10.1029/2007JD008684.

(3) Congress, U. S. CAAA90 Clean Air Act Amendments of 1990. Public Law 549, 1990.

(4) Ministry of Environmental Protection, Airborne Pollution Prevention and Control Action Plan (2013–17); http://zfs.mep.gov.cn/fg/gwyw/201309/t20130912_260045.htm (accessed September 20, 2016).

(5) Reanalysis of the tropospheric chemical composition over the past 40 years (RETRO); http://retro-archive.iek.fz-juelich.de/ (accessed october 13, 2015).

(6) Emission Database for Global Atmospheric Research, release version 4.3.1 (EDGAR_v4.3.1); http://edgar.jrc.ec.europa.eu (accessed January 11, 2017).

(7) European Monitoring and Evaluation Programme (EMEP); http://webdab1.umweltbundesamt.at/cgi-bin/wedb2_controller.pl (accessed March 5, 2017).

(8) International Energy Agency (IEA) World Energy Statistics and Balances; http://www.oecd-ilibrary.org/statistics (accessed Octorber 10, 2016).

(9) Kurokawa, J.; Ohara, T.; Morikawa, T.; Hanayama, S.; Janssens-Maenhout, G.; Fukui, T.; Kawashima, K.; Akimoto, H. Emissions of air pollutants and greenhouse gases over Asian regions during 2000–2008: Regional Emission inventory in ASia (REAS) version 2. *Atmos. Chem. Phys.* **2013**, *13* (21), 11019–11058.

(10) Lamarque, J. F.; Bond, T. C.; Eyring, V.; Granier, C.; Heil, A.; Klimont, Z.; Lee, D.; Liousse, C.; Mieville, A.; Owen, B.; Schultz, M. G.; Shindell, D.; Smith, S. J.; Stehfest, E.; Van Aardenne, J.; Cooper, O. R.; Kainuma, M.; Mahowald, N.; McConnell, J. R.; Naik, V.; Riahi, K.; van Vuuren, D. P. Historical (1850–2000) gridded anthropogenic and biomass burning emissions of reactive gases and aerosols: methodology and application. *Atmos. Chem. Phys.* **2010**, *10* (15), 7017–7039.

(11) Ohara, T.; Akimoto, H.; Kurokawa, J.; Horii, N.; Yamaji, K.; Yan, X.; Hayasaka, T. An Asian emission inventory of anthropogenic emission sources for the period 1980–2020. *Atmos. Chem. Phys.* **2007**, *7* (16), 4419–4444.

(12) Streets, D. G.; Bond, T. C.; Carmichael, G. R.; Fernandes, S. D.; Fu, Q.; He, D.; Klimont, Z.; Nelson, S. M.; Tsai, N. Y.; Wang, M. Q.; Woo, J. H.; Yarber, K. F., An inventory of gaseous and primary aerosol emissions in Asia in the year 2000. *J. Geophys. Res.: Atmos.* **2003**, *108*, (D21).10.1029/2002JD003093

(13) Zhao, B.; Wang, S. X.; Liu, H.; Xu, J. Y.; Fu, K.; Klimont, Z.; Hao, J. M.; He, K. B.; Cofala, J.; Amann, M. NOx emissions in China: historical trends and future perspectives. *Atmos. Chem. Phys.* **2013**, *13* (19), 9869–9897.

(14) Emmons, L. K.; Walters, S.; Hess, P. G.; Lamarque, J. F.; Pfister, G. G.; Fillmore, D.; Granier, C.; Guenther, A.; Kinnison, D.; Laepple, T.; Orlando, J.; Tie, X.; Tyndall, G.; Wiedinmyer, C.; Baughcum, S. L.; Kloster, S. Description and evaluation of the Model for Ozone and Related chemical Tracers, version 4 (MOZART-4). *Geosci. Model Dev.* **2010**, *3* (1), 43–67.

(15) Li, X. Y.; Liu, J. F.; Mauzerall, D. L.; Emmons, L. K.; Walters, S.; Horowitz, L. W.; Tao, S. Effects of trans-Eurasian transport of air pollutants on surface ozone concentrations over Western China. *J. Geophys. Res.: Atmos.* **2014**, *119* (21), 12338–12354.

(16) Present and future surface emissions of atmospheric compounds (POET); http://eccad.sedoo.fr/eccad_extract_interface/doc/pdf/POET_documentation.pdf (accessed May 5, 2016).

(17) Wang, R.; Tao, S.; Ciais, P.; Shen, H. Z.; Huang, Y.; Chen, H.; Shen, G. F.; Wang, B.; Li, W.; Zhang, Y. Y.; Lu, Y.; Zhu, D.; Chen, Y. C.; Liu, X. P.; Wang, W. T.; Wang, X. L.; Liu, W. X.; Li, B. G.; Piao, S. L. High-resolution mapping of combustion processes and implications for CO2 emissions. *Atmos. Chem. Phys.* **2013**, *13* (10), 5189–5203.

(18) Chen, Y. L.; Wang, R.; Shen, H. Z.; Li, W.; Chen, H.; Huang, Y.; Zhang, Y. Y.; Chen, Y. C.; Su, S.; Lin, N.; Liu, J.; Li, B. G.; Wang, X. L.; Liu, W. X.; Coveney, R. M.; Tao, S. Global Mercury Emissions from Combustion in Light of International Fuel Trading. *Environ. Sci. Technol.* **2014**, *48* (3), 1727–1735.

DOI: 10.1021/acs.est.7b02235
Environ. Sci. Technol. 2017, 51, 7992−8000

(19) Huang, Y.; Shen, H. Z.; Chen, H.; Wang, R.; Zhang, Y. Y.; Su, S.; Chen, Y. C.; Lin, N.; Zhuo, S. J.; Zhong, Q. R.; Wang, X. L.; Liu, J. F.; Li, B. G.; Liu, W. X.; Tao, S. Quantification of Global Primary Emissions of PM2.5, PM10, and TSP from Combustion and Industrial Process Sources. *Environ. Sci. Technol.* **2014**, *48* (23), 13834−13843.
(20) Meng, W. J.; Zhong, Q. R.; Yun, X.; Zhu, X.; Huang, T. B.; Shen, H. Z.; Chen, Y. L.; Chen, H.; Zhou, F.; Liu, J. F.; Wang, X. M.; Zeng, E. Y.; Tao, S. Improvement of a Global High-Resolution Ammonia Emission Inventory for Combustion and Industrial Sources with New Data from the Residential and Transportation Sectors. *Environ. Sci. Technol.* **2017**, *51* (5), 2821−2829.
(21) Shen, H. Z.; Huang, Y.; Wang, R.; Zhu, D.; Li, W.; Shen, G. F.; Wang, B.; Zhang, Y. Y.; Chen, Y. C.; Lu, Y.; Chen, H.; Li, T. C.; Sun, K.; Li, B. G.; Liu, W. X.; Liu, J. F.; Tao, S. Global Atmospheric Emissions of Polycyclic Aromatic Hydrocarbons from 1960 to 2008 and Future Predictions. *Environ. Sci. Technol.* **2013**, *47* (12), 6415−6424.
(22) Wang, R.; Tao, S.; Shen, H. Z.; Huang, Y.; Chen, H.; Balkanski, Y.; Boucher, O.; Ciais, P.; Shen, G. F.; Li, W.; Zhang, Y. Y.; Chen, Y. C.; Lin, N.; Su, S.; Li, B. G.; Liu, J. F.; Liu, W. X. Trend in Global Black Carbon Emissions from 1960 to 2007. *Environ. Sci. Technol.* **2014**, *48* (12), 6780−6787.
(23) Zhong, Q. R.; Huang, Y.; Shen, H. Z.; Chen, Y. L.; Chen, H.; Huang, T. B.; Zeng, E. Y.; Tao, S. Global estimates of carbon monoxide emissions from 1960 to 2013. *Environ. Sci. Pollut. Res.* **2017**, *24* (1), 864−873.
(24) Chen, H.; Huang, Y.; Shen, H. Z.; Chen, Y. L.; Ru, M. Y.; Chen, Y. C.; Lin, N.; Su, S.; Zhuo, S. J.; Zhong, Q. R.; Wang, X. L.; Liu, J. F.; Li, B. G.; Tao, S. Modeling temporal variations in global residential energy consumption and pollutant emissions. *Appl. Energy* **2016**, *184*, 820−829.
(25) Wang, R.; Tao, S.; Shen, H. Z.; Wang, X. L.; Li, B. G.; Shen, G. F.; Wang, B.; Li, W.; Liu, X. P.; Huang, Y.; Zhang, Y. Y.; Lu, Y.; Ouyang, H. L. Global Emission of Black Carbon from Motor Vehicles from 1960 to 2006. *Environ. Sci. Technol.* **2012**, *46* (2), 1278−1284.
(26) Bond, T. C.; Bhardwaj, E.; Dong, R.; Jogani, R.; Jung, S. K.; Roden, C.; Streets, D. G.; Trautmann, N. M., Historical emissions of black and organic carbon aerosol from energy-related combustion, 1850−2000. *Global Biogeochem. Cycles* **2007**, *21*, (2). DOI: n/a10.1029/2006GB002840.
(27) Tao, S.; Ru, M. Y.; Du, W.; Zhu, X.; Zhong, Q. R.; Li, B. G.; Shen, G. F.; Pan, X. L.; Meng, W. J.; Chen, Y. L.; Shen, H. Z.; Lin, N.; Su, S.; Zhuo, S. J.; Huang, T. B.; Xu, Y.; Liu, J. F.; Wang, X. L.; Liu, W. X.; Cheng, H. F.; Zhu, D. Q., Environmental, Health, and Climate Co-benefits of the Rural Residential Energy Transition in China, submitted.
(28) Global Fire Emissions Database (verson 4 including small fires, GFEDv4s); http://www.globalfiredata.org/data.html (accessed Octorber 13, 2015).
(29) World Steel Association; http://www.worldsteel.org (accessed October 24, 2015).
(30) U. S. Geological Survey (USGS) Commodity Statistics and Information; http://minerals.usgs.gov/minerals/pubs/commodity (accessed September 23, 2015).
(31) Endresen, O.; Sorgard, E.; Behrens, H. L.; Brett, P. O.; Isaksen, I. S. A., A historical reconstruction of ships' fuel consumption and emissions. *J. Geophys. Res.* **2007**, *112*, (D12). DOI: 10.1029/2006JD007630.
(32) Yan, F.; Winijkul, E.; Jung, S.; Bond, T. C.; Streets, D. G. Global emission projections of particulate matter (PM): I. Exhaust emissions from on-road vehicles. *Atmos. Environ.* **2011**, *45* (28), 4830−4844.
(33) Wojtowicz, M. A.; Pels, J. R.; Moulijn, J. A. N2o Emission Control in Coal Combustion. *Fuel* **1994**, *73* (9), 1416−1422.
(34) Eyring, V.; Kohler, H. W.; van Aardenne, J.; Lauer, A., Emissions from international shipping: 1. The last 50 years. *J. Geophys. Res.* **2005**, *110*, (D17).10.1029/2004JD005619
(35) Winther, M.; Christensen, J. H.; Plejdrup, M. S.; Ravn, E. S.; Eriksson, O. F.; Kristensen, H. O. Emission inventories for ships in the arctic based on satellite sampled AIS data. *Atmos. Environ.* **2014**, *91*, 1−14.
(36) World Bank Country and Lending Groups, https://datahelpdesk.worldbank.org/knowledgebase/articles/906519-world-bank-country-and-lending-groups (accessed July 6, 2016).
(37) OICA International Organization of Motor Vehicle Manufacturers; http://www.oica.net/ (accessed March 11, 2017).
(38) World Bank Open Data; http://data.worldbank.org.cn/ (accessed October 25, 2016).
(39) Ru, M. Y.; Zhong, Q. R.; Tao, S.; Shindell, D., Emission Trajectories of BC Compared to CO2 and SO2 Based on Global Country-level Emission Inventories, submitted.
(40) Selden, T. M.; Song, D. Environmental quality and development: is there a Kuznets curve for air pollution emissions? *J. Environ. Econ. Manage.* **1994**, *27* (2), 147−162.
(41) Shen, H. Z.; Tao, S.; Chen, Y. L.; Ciais, P.; Güneralp, B.; Ru, M. Y.; Zhong, Q. R.; Yun, X.; Zhu, X.; Huang, T. B.; Tao, W.; Chen, Y. C.; Li, B. G.; Wang, X. L.; Liu, W. X.; Liu, J. F.; Zhao, S. Q. Urbanization-induced population migration has reduced ambient PM2.5 concentrations in China, *Science Advances*, in press.
(42) National Bureau of Statistics of China (NBSC). *China Statistical Yearbook 2000−2014*; China Statistics Press: Beijing, 2014.
(43) Liu, F.; Zhang, Q.; Ronald, J. V.; Zheng, B.; Tong, D.; Yan, L.; Zheng, Y. X.; He, K. B., Recent reduction in NOx emissions over China: synthesis of satellite observations and emission inventories. *Environ. Res. Lett.* **2016**, *11*, (11). DOI: 11400210.1088/1748-9326/11/11/114002.
(44) ECCAD Emission of atmospheric compounds & compilation of ancillary Data; http://eccad.sedoo.fr/eccad_extract_interface/JSF/page_login.jsf (accessed March 1, 2017).
(45) Verbong, G.; Geels, F. The ongoing energy transition: Lessons from a socio-technical, multi-level analysis of the Dutch electricity system (1960−2004). *Energy Policy* **2007**, *35* (2), 1025−1037.
(46) Su, S. S.; Li, B. G.; Cui, S. Y.; Tao, S. Sulfur Dioxide Emissions from Combustion in China: From 1990 to 2007. *Environ. Sci. Technol.* **2011**, *45* (19), 8403−8410.
(47) Hebei Environmental Protection Bureau, Emission standard of air pollutants for iron and steel industry, DB13/2169−2015, 2015.2.
(48) Ministry of Environmental Protection, Emission standard of air pollutants from thermal power plants, GB 13223−2011, 2012,3.
(49) Giglio, L.; Randerson, J. T.; van der Werf, G. R. Analysis of daily, monthly, and annual burned area using the fourth-generation global fire emissions database (GFED4). *J. Geophys. Res.: Biogeosci.* **2013**, *118* (1), 317−328.
(50) van der Werf, G. R.; Randerson, J. T.; Giglio, L.; Collatz, G. J.; Mu, M.; Kasibhatla, P. S.; Morton, D. C.; DeFries, R. S.; Jin, Y.; van Leeuwen, T. T. Global fire emissions and the contribution of deforestation, savanna, forest, agricultural, and peat fires (1997−2009). *Atmos. Chem. Phys.* **2010**, *10* (23), 11707−11735.
(51) Emission Database for Global Atmospheric Research, release version 4.2 (EDGAR_v4.2); http://edgar.jrc.ec.europa.eu (accessed January 11, 2017).
(52) Eyring, V.; Isaksen, I. S. A.; Berntsen, T.; Collins, W. J.; Corbett, J. J.; Endresen, O.; Grainger, R. G.; Moldanova, J.; Schlager, H.; Stevenson, D. S. Transport impacts on atmosphere and climate: Shipping. *Atmos. Environ.* **2010**, *44* (37), 4735−4771.
(53) Jaegle, L.; Steinberger, L.; Martin, R. V.; Chance, K. Global partitioning of NOx sources using satellite observations: Relative roles of fossil fuel combustion, biomass burning and soil emissions. *Faraday Discuss.* **2005**, *130*, 407−423.
(54) Richter, A.; Burrows, J. P.; Nuss, H.; Granier, C.; Niemeier, U. Increase in tropospheric nitrogen dioxide over China observed from space. *Nature* **2005**, *437* (7055), 129−132.
(55) Stavrakou, T.; Muller, J. F.; Boersma, K. F.; De Smedt, I.; van der A, R. J., Assessing the distribution and growth rates of NOx emission sources by inverting a 10-year record of NO2 satellite columns. *Geophys. Res. Lett.* **2008**, *35*, (10). DOI: 10.1029/2008GL033521.

DOI: 10.1021/acs.est.7b02235
Environ. Sci. Technol. 2017, 51, 7992−8000

(56) Uno, I.; He, Y.; Ohara, T.; Yamaji, K.; Kurokawa, J. I.; Katayama, M.; Wang, Z.; Noguchi, K.; Hayashida, S.; Richter, A.; Burrows, J. P. Systematic analysis of interannual and seasonal variations of model-simulated tropospheric NO2 in Asia and comparison with GOME-satellite data. *Atmos. Chem. Phys.* **2007**, *7* (6), 1671−1681.
(57) Miyazaki, K.; Eskes, H.; Sudo, K.; Boersma, K. F.; Bowman, K.; Kanaya, Y. Decadal changes in global surface NOx emissions from multi-constituent satellite data assimilation. *Atmos. Chem. Phys.* **2017**, *17* (2), 807−837.
(58) de Foy, B.; Lu, Z. F.; Streets, D. G., Satellite NO2 retrievals suggest China has exceeded its NOx reduction goals from the twelfth Five-Year Plan. *Sci. Rep.* **2016**, *6*. DOI: 10.1038/srep35912.
(59) Popp, D. *Exploring Links between Innovation and Diffusion: Adoption of NOx Control Technologies at US Coal-Fired Power Plants*; National Bureau of Economic Research, 2006.
(60) Ban-Weiss, G. A.; McLaughlin, J. P.; Harley, R. A.; Lunden, M. M.; Kirchstetter, T. W.; Kean, A. J.; Strawa, A. W.; Stevenson, E. D.; Kendall, G. R. Long-term changes in emissions of nitrogen oxides and particulate matter from on-road gasoline and diesel vehicles. *Atmos. Environ.* **2008**, *42* (2), 220−232.
(61) Dallmann, T. R.; Harley, R. A., Evaluation of mobile source emission trends in the United States. *J. Geophys. Res.* **2010**, *115*. DOI: 10.1029/2010JD013862.
(62) Harley, R. A.; Marr, L. C.; Lehner, J. K.; Giddings, S. N. Changes in motor vehicle emissions on diurnal to decadal time scales and effects on atmospheric composition. *Environ. Sci. Technol.* **2005**, *39* (14), 5356−5362.
(63) Dargay, J.; Gately, D.; Sommer, M. Vehicle ownership and income growth, worldwide: 1960−2030. *Energy J.* **2007**, *28* (4), 143−170.
(64) Wu, T.; Zhao, H. M.; Ou, X. M. Vehicle Ownership Analysis Based on GDP per Capita in China: 1963−2050. *Sustainability* **2014**, *6* (8), 4877−4899.
(65) Chen, Y. L.; Shen, H. Z.; Zhong, Q. R.; Chen, H.; Huang, T. B.; Liu, J. F.; Cheng, H. F.; Zeng, E. Y.; Smith, K. R.; Tao, S. Transition of household cookfuels in China from 2010 to 2012. *Appl. Energy* **2016**, *184*, 800−809.
(66) Wang, H. K.; Fu, L. X.; Zhou, Y.; Du, X.; Ge, W. H. Trends in vehicular emissions in China's mega cities from 1995 to 2005. *Environ. Pollut.* **2010**, *158* (2), 394−400.
(67) Wang, X.; Westerdahl, D.; Hu, J. N.; Wu, Y.; Yin, H.; Pan, X. C.; Zhang, K. M. On-road diesel vehicle emission factors for nitrogen oxides and black carbon in two Chinese cities. *Atmos. Environ.* **2012**, *46*, 45−55.
(68) Yanowitz, J.; McCormick, R. L.; Graboski, M. S. In-use emissions from heavy-duty diesel vehicles. *Environ. Sci. Technol.* **2000**, *34* (5), 729−740.
(69) JC08; http://transportpolicy.net/index.php?title=Japan:_Light-duty:_JC08 (accessed March 1, 2017).
(70) Ministry of Environmental Protection, Limits and measurement methods for emissions from light-duty vehicles(CHINA 5); http://kjs.mep.gov.cn/hjbhbz/bzwb/dqhjbh/dqydywrwpfbz/201309/t20130917_260352.htm (accessed February 1, 2017).
(71) Cole, M. A.; Rayner, A. J.; Bates, J. M. The environmental Kuznets curve: an empirical analysis. *Environ. Dev. Econ.* **1997**, *2* (04), 401−416.

DOI: 10.1021/acs.est.7b02235
Environ. Sci. Technol. 2017, 51, 7992−8000